J|A|C|S
ARTICLES
Published on Web 12/04/2007

Supramolecular Carbon Nanotube-Fullerene Donor−Acceptor Hybrids for Photoinduced Electron Transfer

Francis D'Souza,*,† Raghu Chitta,† Atula S. D. Sandanayaka,‡ Navaneetha K. Subbaiyan,† Lawrence D'Souza,§ Yasuyuki Araki,‡ and Osamu Ito*,‡

Department of Chemistry, Wichita State University, 1845 Fairmount, Wichita, Kansas 67260-0051, Institute of Multidisciplinary Research for Advanced Materials, Tohoku University, Katahira, Sendai, 980-8577, Japan, and Department of Chemical Engineering, University of Illinois at Chicago, 810 South Clinton, Chicago, Illinois 60607

Received June 5, 2007; E-mail: Francis.DSouza@wichita.edu; ito@tagen.tohoku.ac.jp

Abstract: Photoinduced electron transfer in a self-assembled single-wall carbon nanotube (SWNT)-fullerene-(C_{60}) hybrid with SWNT acting as an electron donor and fullerene as an electron acceptor has been successfully demonstrated. Toward this, first, SWNTs were noncovalently functionalized using alkyl ammonium functionalized pyrene (Pyr-NH_3^+) to form SWNT/Pyr-NH_3^+ hybrids. The alkyl ammonium entity of SWNT/Pyr-NH_3^+ hybrids was further utilized to complex with benzo-18-crown-6 functionalized fullerene, crown-C_{60}, via ammonium−crown ether interactions to yield SWNT/Pyr-NH_3^+/crown-C_{60} nanohybrids. The nanohybrids were isolated and characterized by TEM, UV−visible−near IR, and electrochemical methods. Free-energy calculations suggested possibility of electron transfer from the carbon nanotube to the singlet excited fullerene in the SWNT/Pyr-NH_3^+/crown-C_{60} nanohybrids. Accordingly, steady-state and time-resolved fluorescence studies revealed efficient quenching of the singlet excited-state of C_{60} in the nanohybrids. Further studies involving nanosecond transient absorption studies confirmed electron transfer to be the quenching mechanism, in which the electron-transfer product, fullerene anion radical, was possible to spectrally characterize. The rates of charge separation, k_{CS}, and charge recombination, k_{CR}, were found to be 3.46×10^9 and 1.04×10^7 s^{-1}, respectively. The calculated lifetime of the radical ion-pair was found to be over 100 ns, suggesting charge stabilization in the novel supramolecular nanohybrids. The present nanohybrids were further utilized to reduce hexyl-viologen dication (HV^{2+}) and a sacrificial electron donor, 1-benzyl-1,4-dihydronicotinamide, in an electron-pooling experiment, offering additional proof for the occurrence of photoinduced charge-separation and potential utilization of these materials in light-energy harvesting applications.

1. Introduction

Carbon nanotubes[1] possessing functional components on their surface, useful for medicinal,[2] electronic,[3] and light-energy harvesting applications,[4] are a topic of current research interest. However, functionalization without irreversible damaging of their electronic structure remains a challenge.[5] In this context, noncovalent functionalization of carbon nanotubes seems to be promising because it not only preserves the electronic structures but also limits severe chemical, thermal, and sonication damages to the tubes. Among the available noncovalent functionalization approaches, the $\pi-\pi$ stacking of macrocyclic compounds[6] on the nanotube surface is found to be a viable approach although further improvements to stabilize resulting conjugate and solubilize without destroying conjugate structure are needed for complete exploitation of the resulting novel materials for different applications.

The excited-state properties of nanohybrids formed between tetrapyrroles and single-wall carbon nanotubes, connected either by covalent linkages or self-assembled via noncovalent methods, have provided evidence for donor−acceptor interactions.[7−9] In the majority of these studies, the single-wall carbon nanotubes (SWNTs) acted as electron acceptors, except in two instances where they were treated as electron donors.[10] However, even using the sophisticated transient absorption methods, it was difficult to spectrally characterize the electron-transfer products

† Wichita State University.
‡ Tohoku University.
§ University of Illinois at Chicago.

(1) (a) Iijima, S. *Nature* **1991**, *354*, 56−58. (b) Iijima, S.; Yudasaka, M.; Yamada, R.; Bandow, S.; Suenaga, K.; Kokai, F.; Takahashi, K. *Chem. Phys. Lett*. **1999**, *309*, 165−170.
(2) (a) Kam, N. W. S.; Liu, Z.; Dai, H. *J. Am. Chem. Soc.* **2005**, *127*, 12492−12493. (b) Sano, M.; Kamino, A.; Okamura, J.; Shinkai, S. *Nano Lett.* **2002**, *2*, 531−533. (c) Singh, R.; Pantarotto, D.; McCarthy, D.; Chaloin, O.; Hoebeke, J. P.; Charalambos, D.; Briand, J.-P.; Prato, M.; Bianco, A.; Kostarelos, K. *J. Am. Chem. Soc.* **2005**, *127*, 4388−4396.
(3) Chichak, K. S.; Star, A.; Altoe, M.; Virginia, P.; Stoddart, J. F. *Small* **2005**, *1*, 452−461.
(4) (a) Guldi, D. M.; Rahman, G. M. A.; Zerbetto, F.; Prato, M. *Acc. Chem. Res.* **2005**, *38*, 871−878. (b) Guldi, D. M.; Taieb, H.; Rahman, G. M. A.; Tagmatarchis, N.; Prato, M. *Adv. Mater.* **2005**, *17*, 871−875. (c) Kamat, P. V. *J. Phys. Chem. C* **2007**, *111*, 2834−2860.
(5) (a) *Carbon Nanotubes: Synthesis, Structure and Applications*; Dresselhaus, M. S., Dresselhaus, G., Avouris, Ph., Eds.; Springer Publishing: New York, 2001. (b) Reich, S.; Thomsen, C.; Maultzsch, J. *Carbon Nanotubes: Basic Concepts and Physical Properties*; Wiley-VCH: Weinheim, 2004.
(6) Chen, R. J.; Zhang, Y.; Wang, D.; Dai, H. *J. Am. Chem. Soc.* **2001**, *123*, 3838−3839.

Scheme 1

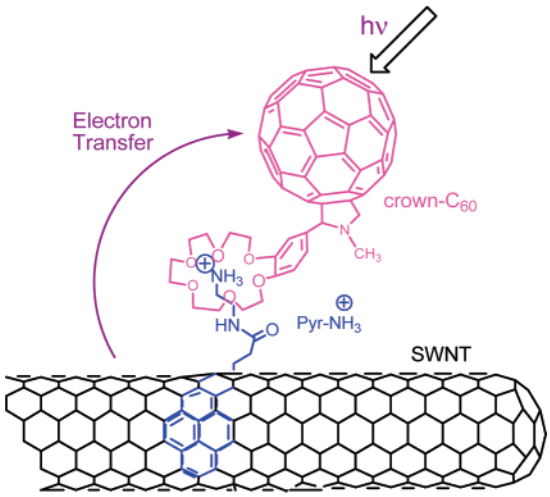

for reasons of lack of clear anion or cation radical signals or overlap of the radical ion absorption peaks with the intense triplet absorption bands. Achieving clear spectral characterization is important to evaluate the lifetimes of the charge-separated states, a property that finally determines the usefulness of these conjugates for light-energy harvesting and photovoltaic applications,[11a] although the charge-transfer dynamics may vary in solid film compared to that in solution.[11b]

In the present study, we have utilized a self-assembly approach involving both $\pi-\pi$ and ammonium−crown ether interactions[12] to obtain stable SWNT−C_{60} nanohybrids, in which radical ion species of C_{60} show genuine absorption bands in the NIR region. Scheme 1 illustrates the methodology adopted for building the SWNT−C_{60} nanohybrids using alkyl ammonium functionalized pyrene (Pyr-NH_3^+) and benzo-18-crown-6 functionalized fullerene, crown-C_{60}. This involves, first, solubilization of SWNTs by treating them with Pyr-NH_3^+. Stacking pyrene entities on the nanotube surface makes the nanotubes soluble without perturbing the electronic structures.[6] Next, the ammonium groups of SWNT/Pyr-NH_3^+ were self-assembled to crown ether appended fullerenes via alkyl ammonium−crown ether complexation, finally generating SWNT/Pyr-NH_3^+/crown-C_{60} nanohybrids. As discussed in the subsequent sections, it was possible to isolate the SWNT/Pyr-NH_3^+/crown-C_{60} nanohybrids and characterize them prior to performing the electrochemical and photochemical studies. Recently, we successfully utilized the alkyl ammonium−crown ether binding self-assembly protocol to obtain stable porphyrin−fullerene conjugates[13] and porphyrin−SWNT nanohybrids.[14] In these systems, photoinduced electron transfer from the singlet excited zinc porphyrin to C_{60} or SWNT was demonstrated. As is revealed here, in the SWNT/Pyr-NH_3^+/crown-C_{60} nanohybrids, the SWNT acts as an electron donor to the singlet excited fullerene generating SWNT$^{\bullet+}$/Pyr-NH_3^+/crown-$C_{60}^{\bullet-}$ as the final charge-separated product with relatively long lifetime.

2. Results and Discussion

2.1. Preparation of SWNT/Pyr-NH_3^+ and SWNT/Pyr-NH_3^+/crown-C_{60}. Purified SWNT (HiPCO, 1.8 mg) and Pyr-NH_3^+ (3.7 mg) were dissolved in dry DMF (15 mL), and the reaction mixture was stirred for 48 h at room temperature. The resulting mixture was sonicated for 6 h at 20 °C, and the resulting slurry was removed. After centrifugation for 2 h, the excess of Pyr-NH_3^+ was removed by separating the yellow color centrifugate from the black precipitate (SWNT/Pyr-NH_3^+). This process was repeated (at least twice) until the solution in centrifuge tube turned colorless. This homogeneous black dispersion in DMF was stable at room temperature. SWNT/Pyr-NH_3^+/crown-C_{60} was obtained by adding crown-C_{60} to SWNT/Pyr-NH_3^+ in DMF; the excess crown-$C_{60}$was removed by adding excess (n-Bu_4N)ClO_4 and agitation of nitrogen gas, which precipitated SWNT/Pyr-NH_3^+/crown-C_{60} as a result of a salt effect. The precipitates collected by centrifugation were washed several times with the solvent to remove any unbound C_{60}-crown and were redissolved in DMF solution for further studies. Direct treatment of SWNT with crown-C_{60} did not result in any precipitation, indicating the importance of the linker Pyr-NH_3^+ in the generation (precipitation) of the nanohybrids. The binding constant evaluated for Pyr-NH_3^+ inserting to crown-C_{60} in DMF was found to be 8.1×10^3 M^{-1}, indicating crown ether−alkyl ammonium ion binding as a viable self-assembly approach.

2.2. Steady-State Absorption Spectra. Figure 1 shows the optical absorption spectrum of SWNT/Pyr-NH_3^+ in the UV−visible−NIR region in DMF. Absorption bands corresponding

(7) (a) Li, H.; Zhou, B.; Lin, Y.; Gu, L.; Wang, W.; Fernando, K. A. S.; Kumar, S.; Allard, L. F.; Sun, Y.-P. *J. Am. Chem. Soc.* **2004**, *126*, 1014−1015. (b) Guldi, D. M.; Taieb, H.; Rahman, G. M. A.; Tagmatarchis, N.; Prato, M. *Adv. Mater.* **2005**, *17*, 871−875. (c) Satake, A.; Miyajima, Y.; Kobuke, Y. *Chem. Mater.* **2005**, *17*, 716−724. (d) Chen, J.; Collier, C. P. *J. Phys. Chem. B* **2005**, *109*, 7605−7609. (e) Hasobe, T.; Fukuzumi, S.; Kamat, P. V. *J. Phys. Chem. B* **2006**, *110*, 25477−25484. (f) Hasobe, T.; Fukuzumi, S.; Kamat, P. V. *Angew. Chem., Int. Ed.* **2006**, *45*, 755−759. (g) Robel, I.; Bunker, B. A.; Kamat, P. V. *Adv. Mater.* **2005**, *17*, 2458−2463.
(8) (a) Li, H.; Martin, R. B.; Harruff, B. A.; Carino, R. A.; Sun, Y.-P. *Adv. Mater.* **2004**, *16*, 896−900. (b) Baskaran, D.; Mays, J. W.; Zhang, X. P.; Bratcher, M. S. *J. Am. Chem. Soc.* **2005**, *127*, 6916−6917. (c) Alvaro, M.; Atienzar, P.; de la Cruz, P.; Delgado, J. L.; Troiani, V.; Garcia, H.; Langa, F.; Palkar, A.; Echegoyen, L. *J. Am. Chem. Soc.* **2006**, *128*, 6626−6635. (d) Herranz, A.; Martin, N.; Campidelli, S.; Prato, M.; Brehm, G.; Guldi, D. M. *Angew. Chem., Int. Ed.* **2006**, *45*, 4478−4482. (e) Guo, Z.; Du, F.; Ren, D.; Chen, Y.; Zheng, J.; Liu, Z.; Tian, J. *J. Mater. Chem.* **2006**, *16*, 3021−3030. (f) Ballesteros, B.; de la Torre, G.; Ehli, C.; Rahman, G. M. A.; Agullo-Ruedo, F.; Guldi, D. M.; Torres, T. *J. Am. Chem. Soc.* **2007**, *129*, 5061−5068.
(9) (a) Guldi, D. M.; Rahman, G. M. A.; Ramey, J.; Marcaccio, M.; Paolucci, D.; Paolucci, F.; Qin, S.; Ford, W. T.; Balbinot, D.; Jux, N.; Tagmatarchis, N.; Prato, M. *Chem. Commun.* **2004**, *18*, 2034−2035. (b) Guldi, D. M.; Rahman, G. M. A.; Jux, N.; Tagmatarchis, N.; Prato, M. *Angew. Chem., Int. Ed.* **2004**, *43*, 5526−5530. (c) Guldi, D. M.; Rahman, G. M. A.; Prato, M.; Jux, N.; Qin, S.; Ford, W. T. *Angew. Chem., Int. Ed.* **2005**, *44*, 2015−2018. (d) Guldi, D. M.; Rahman, G. M. A.; Qin, S.; Tchoul, M.; Ford, W. T.; Marcaddio, M.; Paolucci, D.; Paolucci, F.; Campidelli, S.; Prato, M. *Chem.−Eur. J.* **2006**, *12*, 2152−2161. (e) Guldi, D. M.; Menna, E.; Maggini, M.; Marcaccio, M.; Paolucci, D.; Paolucci, F.; Campidelli, S.; Prato, M.; Rahman, G. M.; Shergna, S. *Chem.−Eur. J.* **2006**, *12*, 3975−3983. (f) Saito, K.; Troiani, V.; Qin, H.; Solladie, N.; Sakata, T.; Mori, H.; Ohama, M.; Fukuzumi, S. *J. Phys. Chem. C.* **2007**, *111*, 1194−1199. (g) Chitta, R.; Sandanayaka, A. S. D.; Schumacher, A. L.; D' Souza, L.; Araki, Y.; Ito, O.; D'Souza, F. *J. Phys. Chem. C* **2007**, *111*, 6947−6955.
(10) (a) Hecht, D. S.; Ramirez, R. J. A.; Briman, M.; Artukovic, E.; Chichak, K. S.; Stoddart, J. F.; Grüner, G. *Nano Lett.* **2006**, *6*, 2031−2036. (b) Boul, P. J.; Cho, D.-G.; Rahman, G. M. A.; Marquez, M.; Ou, Z.; Kadish, K. M.; Guldi, D. M.; Sessler, J. L. *J. Am. Chem. Soc.* **2007**, *129*, 5683−5687.
(11) (a) Verhoeven, J. W. *J. Photochem. Photobiol. C Rev.* **2006**, *7*, 40−60. (b) Handa, S.; Giacalone, F.; Haque, S. A.; Palomares, E.; Martin, N.; Durrant, J. R. *Chem.−Eur. J.* **2005**, *11*, 7440−7447.
(12) El-Khouly, M. E.; Ito, O.; Smith, P. M.; D'Souza, F. *J. Photochem. Photobiol. C* **2004**, *5*, 79−104.
(13) (a) D'Souza, F.; Chitta, R.; Gadde, S.; Zandler, M. E.; Sandanayaka, A. S. D.; Araki, Y.; Ito, O. *Chem. Commun.* **2005**, 1279−1281. (b) D'Souza, F.; Chitta, R.; Gadde, S.; Zandler, M. E.; McCarty, A. L.; Sandanayaka, A. S. D.; Araki, Y.; Ito, O. *Chem.−Eur. J.* **2005**, *11*, 4416−4428. (c) D'Souza, F.; Chitta, R.; Gadde, S.; Islam, D. M. S.; Schumacher, A. L.; Zandler, M. E.; Araki, Y.; Ito, O. *J. Phys. Chem. B.* **2006**, *110*, 25240−25250. (d) D'Souza, F.; Chitta, R.; Gadde, S.; Rogers, L. M.; Karr, P. A.; Zandler, M. E.; Sandanayaka, A. S. D.; Araki, Y.; Ito, O. *Chem.−Eur. J.* **2007**, *13*, 916−992.
(14) D'Souza, F.; Chitta, R.; Sandanayaka, A. S. D.; Subbaiyan, N. K.; D'Souza, L.; Araki, Y.; Ito, O. *Chem.−Eur. J.* **2007**, *13*, 8277−8284.

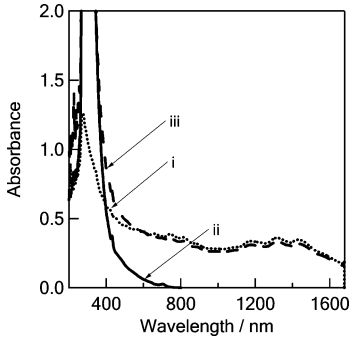

Figure 1. Steady-state absorption spectrum of (i) SWNT/Pyr-NH_3^+, (ii) crown-C_{60}, and (iii) SWNT/Pyr-NH_3^+/crown-C_{60} nanohybrids in DMF.

to the metallic SWNT (400−600 nm region corresponding to M_{11} transitions) and semiconducting SWNT (600−950 nm corresponding to S_{22} transitions and 1100−1600 nm corresponding to S_{11} transitions)[15] were observed. The fine structures of the absorptions indicate preserving the electronic structure of the SWNT after noncovalent interaction with Pyr-NH_3^+. In the UV region, the samples also revealed peaks corresponding to the pyrene entities. However, these bands were found to be broadened as compared to pristine Pyr-NH_3^+ bands due to π-stacking with the SWNTs. The presence of stacked pyrene entity on SWNT was also confirmed by the Pyr-fluorescence quenching of SWNT/Pyr-NH_3^+ in the 375−430 nm range in DMF as a consequence of $\pi-\pi$ interaction stacking of pyrene with the SWNT surface (see Figure S1 in the Supporting Information).[16]

The absorption spectrum of the isolated donor-connector-acceptor nanohybrids, SWNT/Pyr-NH_3^+/crown-C_{60}, in DMF revealed peaks in the visible−near IR region similar to SWNT/Pyr-NH_3^+. In addition, fullerene C_{60} bands in the 300−400 nm region were also observed (Figure 1). Collectively, these observations suggest the existence of SWNT/Pyr-NH_3^+/crown-C_{60} nanohybrids as shown in Scheme 1 in solution.

2.3. TEM Imaging of SWNT/Pyr-NH_3^+/crown-C_{60} Morphology. The TEM images of pristine nanotubes dispersed in DMF solution are shown in Figure 2a. They revealed amorphous carbons and the Fe nanoparticles, which appeared as dark clusters. However, we were able to get rid of most of these impurities upon Pyr-NH_3^+ treatment of the nanotubes.[14] In addition, the SWNT bundles were loosened to some extent by the treatment of Pyr-NH_3^+, although some of them intertwine again during TEM sample preparation. The TEM image of the isolated SWNT/Pyr-NH_3^+/crown-C_{60} hybrid is shown in Figure 2b. Better-defined nanotubes (2−4 nanotubes bundled) were observed. Most likely in the SWNT/Pyr-NH_3^+/crown-C_{60} nanohybrids, the C_{60}-crown occupies the outer surface of the bundled nanotubes.[17]

2.4. Electrochemical Redox Potentials. Probing the redox behavior of carbon nanotubes in a systematic manner has been challenging because of their low electrochemical sensitivity and solubility.[18] Often the problem was as a result of obtaining stable solutions or suspensions under electrochemical conditions containing excess amounts of supporting electrolyte (millimolar quantities) in polar solvents and interference from additives used for solubilization of nanotubes (e.g., surfactants, polymeric chains, etc.). Both cathodic and anodic scannings of the potential resulted in large capacitance-type currents, which were attributed to the superimposition of the voltammetric pattern of several semiconducting SWNTs. Although attempts have been made to assign potential range to carbon nanotube varying in their sizes,[19] no clear Faradic processes were reported for carbon nanotubes.

Figure 3 shows the cyclic voltammograms of SWNT/Pyr-NH_3^+/crown-C_{60} nanohybrids along with that of the control compounds in DMF containing 0.1 M (n-Bu_4N)ClO_4. Pristine C_{60}-crown revealed the first two one-electron reductions at $E_{1/2} = -0.34$ and -0.84 V vs Ag/AgCl. As mentioned earlier, when SWNT/Pyr-NH_3^+ was added to the crown-C_{60} solution in the presence of excess (n-Bu_4N)ClO_4, the resulting SWNT/Pyr-NH_3^+/crown-C_{60}nanohybrid started precipitating out of the solution due to the high ionic strength of the solution and the agitation caused by the nitrogen gas purging. The precipitates, after the workup of removing the unbound crown-C_{60}, were carefully redissolved in degassed DMF solution for electrochemical measurements. The cyclic voltammograms of this nanohybrid are shown in Figure 3 (magenta line). Two reductions at potentials close to that of pristine C_{60}-crown were observed, however, with increased peak-to-peak separation, suggesting the occurrence of relatively slow electron transfer.[20] Additionally, the background currents increased considerably after the first reduction (compared to the background current shown in red line), which may be ascribed to the reduction of carbon nanotubes. The shapes of the voltammograms support close positioning of the C_{60} moiety to the surface of SWNT.

On the anodic side probing oxidation, broad irreversible wave started emerging around +0.71 V vs Ag/AgCl. Control experiments performed on SWNT/Pyr-NH_3^+ without crown-C_{60} (blue line) also confirmed appearance of such wave. The potential range of this wave agreed well with that of literature report for oxidation of pyrene stacked SWNT.[19a] It may be mentioned here that no oxidation or reduction processes for Pyr-NH_3^+ within the employed anodic or cathodic potential range (1.0 to −1.2 V) were observed.

From the electrochemical redox data, the driving forces for charge recombination ($-\Delta G_{CR}$) and charge separation ($-\Delta G_{CS}$)

(15) Hamon, M. A.; Itkis, M. E.; Niyogi, S.; Alvaraez, T.; Kuper, C.; Menon, M.; Haddon, R. C. *J. Am. Chem. Soc.* **2001**, *123*, 11292−11293.
(16) (a) *Principles of Fluorescence Spectroscopy*, 2nd ed.; Lakowicz, J. R., Ed.; Kluwer Academic: New York, 1999. (b) See for pyrene quenching with SWNT: Guldi, D. M.; Marcaccio, M.; Paolucci, D.; Paolucci, F.; Tagmatarchis, N.; Tasis, D.; Vazquez, E.; Prato, M. *Angew. Chem., Int. Ed.* **2003**, *115*, 4206. (c) See for pyrene quenching with CNH: Sandanayaka, A. S. D.; Pagona, G.; Tagmatarchis, N.; Yudasaka, M.; Iijima, S.; Araki, Y.; Ito, O. *J. Mater. Chem.* **2007**, *17*, 2540.
(17) Takaguchi, Y. Y.; Tamura, M.; Sako, Y.; Yanagimoto, Y.; Tsuboi, S.; Uchida, T.; Shimamura, K.; Kimura, S.; Wakahara, T.; Maeda, Y.; Akasaka, T. *Chem. Lett.* **2005**, *34*, 1608.
(18) (a) Sumanasekera, G. U.; Allen, J. L.; Fang, S. L.; Loper, A. L.; Rao, A. M.; Eklund, P. C. *J. Phys. Chem. B* **1999**, *103*, 4292−4297. (b) Kavan, L.; Rapta, P.; Dunsch, L.; Bronikowski, M. J.; Willis, P.; Smalley, R. E. *J. Phys. Chem. B* **2001**, *105*, 10764−10771. (c) Li, J.; Cassell, A.; Delzeit, L.; Han, J.; Meyyappan, M. *J. Phys. Chem. B* **2002**, *106*, 9299−9305. (d) Diao, P.; Liu, Z.; Wu, B.; Nan, X.; Zhang, J.; Wei, Z. *ChemPhysChem* **2002**, *3*, 898−991. (e) Day, T. M.; Unwin, P. R.; Wilson, N. R.; Macpherson, J. V. *J. Am. Chem. Soc.* **2005**, *127*, 10639−10647. (f) Heller, I.; Kong, J.; Williams, K. A.; Dekker, C.; Lemay, S. G. *J. Am. Chem. Soc.* **2006**, *128*, 7353−7359. (g) Zheng, M.; Diner, B. *J. Am. Chem. Soc.* **2004**, *126*, 15490−15494. (h) Dukovic, G.; White, B. E.; Zhou, Z.; Wang, F.; Jockusch, S.; Steigerwald, M. L.; Heinz, T. F.; Friesner, R. A.; Turro, N. J.; Brus, L. E. *J. Am. Chem. Soc.* **2004**, *126*, 15269−15276.
(19) (a) Mello-Franco, M.; Marcaccio, M.; Paolucci, D.; Paolucci, F.; Georgakilas, V.; Guldi, D. M.; Prato, M.; Zerbetto, F. *J. Am. Chem. Soc.* **2004**, *126*, 1646−1647. (b) Ehli, C.; Rahman, G. M. A.; Jux, N.; Balbinot, D.; Guldi, D. M.; Paolucci, F.; Marcaccio, M.; Paolucci, D.; Melle-Franco, M.; Zerbetto, F.; Campidelli, S.; Prato, M. *J. Am. Chem. Soc.* **2006**, *128*, 11222−11231.
(20) *Electrochemical Methods: Fundamentals and Applications*, 2nd ed.; Bard, A. J., Faulkner, L. R., Eds.; John Wiley: New York, 2001.

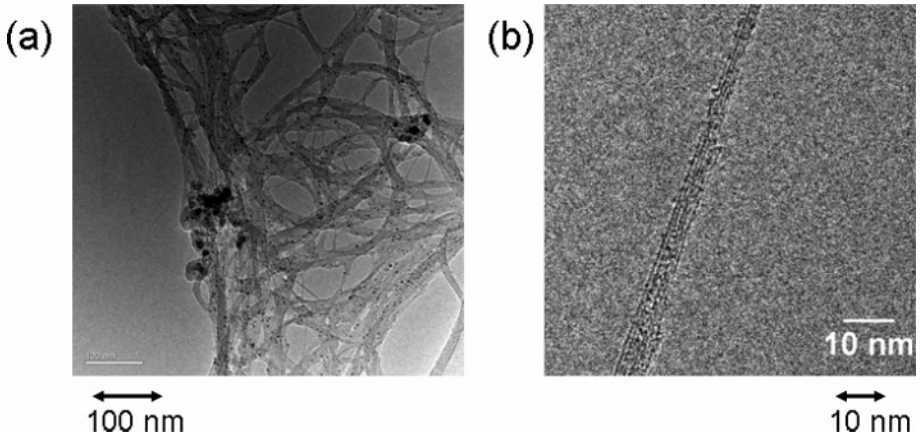

Figure 2. TEM images of (a) pristine SWNT and (b) isolated SWNT/Pyr-NH_3^+/crown-C_{60} conjugate. DMF was initially used to disperse the nanotubes on the grid.

were calculated according to Rehm−Weller relation.[21] The lowest energy of the charge-separated state, which is equal to $-\Delta G_{CR}$, can be approximately calculated from difference between the first reduction potential of crown-C_{60} (−0.34 V) and the oxidation potential of SWNT (+0.71 V as the lowest limit) to be higher than 1.05 eV in DMF. Thus, the ΔG_{CS} value via the singlet excited-state of the C_{60} moiety ($^1C_{60}$*) was calculated to be less than 0.64 eV by employing the lowest $^1C_{60}$*-energy to be 1.70 eV in DMF. The negative ΔG_{CS} and ΔG_{CR} values predict exothermic charge separation from SWNT to $^1C_{60}$* in the SWNT/Pyr-NH_3^+/crown-C_{60} nanohybrids and the exothermic charge recombination in SWNT$^{\bullet+}$/Pyr-NH_3^+/crown-$C_{60}^{\bullet-}$.

2.5. Steady-State and Time-Resolved Fluorescence Studies. The formation of the SWNT/Pyr-NH_3^+/crown-C_{60} nanohybrids was also confirmed by the $^1C_{60}$* fluorescence measurements, which also gives information about the excited-state events in this nanohybrids. Figure 4 shows the fluorescence spectrum of crown-C_{60} in DMF (solid line), exhibiting a peak maximum at 715 nm. Interestingly, in the nanohybrids obtained by the addition of SWNT/Pyr-NH_3^+ to the solution of crown-C_{60}, the peak intensity of the C_{60}-fluorescence was found to be quenched over 80% of its original value (dotted line in Figure 4) suggesting occurrence of excited-state events.[22] As a control experiment, crown-C_{60} was also titrated with Pyr-NH_3^+ having no SWNT. Under these conditions, the fullerene fluorescence was not quenched within an experimental error (<5%), suggesting Pyr-NH_3^+ to be photochemically inactive. These observations confirmed the existence of the SWNT/Pyr-NH_3^+/crown-C_{60} nanohybrids in DMF.

To obtain the kinetic data of fluorescence quenching, picosecond time-resolved emission studies were performed. The time profiles collected in the emission region of the C_{60} are shown in Figure 4b. The emission of crown-C_{60} in DMF followed a monoexponential decay with a lifetime of 1420 ps. Addition of SWNT/Pyr-NH_3^+ to form the nanohybrids accelerated the C_{60}-fluorescence decay, which could be curve-fitted to a biexponential decay function. The C_{60}-fluorescence lifetimes evaluated under these conditions were found to be 240 ps (70%) and 1700 ps (30%), in which the longer lifetime may be attributed to the unbound crown-C_{60}. Because the C_{60}-fluorescence lifetime could not be influenced by the sample concentration, the fast decaying component serves as an additional evidence for the formation of SWNT/Pyr-NH_3^+/crown-C_{60} nanohybrids. By assuming that the fast decaying component is due to electron transfer, the rate of charge separation, k_{CS}, and quantum yield, Φ_{CS}, were evaluated according to eqs 1 and 2:[12]

$$k_{CS} = (1/\tau_f)_{nanohybrid} - (1/\tau_f)_{ref} \quad (1)$$

$$\Phi_{CS} = [(1/\tau_f)_{nanohybrid} - (1/\tau_f)_{ref}]/(1/\tau_f)_{nanohybrid} \quad (2)$$

where $(1/\tau_f)_{nanohybrid}$ and $(1/\tau_f)_{ref}$ are the lifetimes of the fullerene moiety in the presence and absence of SWNT/Pyr-NH_3^+, respectively. The evaluated k_{CS} and Φ_{CS} in DMF were found to be 3.46×10^9 s^{-1} and 0.83, respectively, which are almost the same as porphyrin-crown-C_{60} supramolecules,[13] suggesting efficient charge separation in the investigated supramolecular nanohybrids. On the other hand, the longer fluorescence lifetime with the remaining 30% due to unbound crown-C_{60} suggests its presence as in equilibrium with the bound crown-C_{60} in DMF solution, even though unbound crown-C_{60} was removed in the initial sample preparation.

2.6. Nanosecond Transient Absorption Studies. Evidences for charge separation and the rate of charge recombination, k_{CR}, were obtained from the transient absorption spectral studies using a 532 nm laser, which predominantly excited the C_{60} moiety in addition to SWNTs. Figure 5 shows the nanosecond transient absorption spectra of the SWNT/Pyr-NH_3^+/crown-C_{60} nanohybrids in DMF. Importantly, a transient absorption peak corresponding to the formation of the fulleropyrrolidine anion radical, $C_{60}^{\bullet-}$, around 1020 nm[23] as an evidence for the occurrence of photoinduced charge separation in the supramolecular nanohybrid was observed in addition to the absorption band at 700 nm corresponding to the triplet state of the C_{60} entity ($^3C_{60}$*). Broad absorption bands around 400 and 1400 nm were observed that could correspond to the SWNT$^{+\bullet}$, although further studies are needed to confirm these assignments. Appearance of $^3C_{60}$* with slow decay can be attributed mainly to the unbound crown-C_{60} (dissociated from SWNT/Pyr-NH_3^+/

(21) (a) Rehm, D.; Weller, A. *Isr. J. Chem.* **1970**, *7*, 259. (b) Mataga, N.; Miyasaka, H. In *Electron Transfer*; Jortner, J., Bixon, M., Eds.; John Wiley & Sons: New York, 1999; Part 2, pp 431−496.

(22) If excitation light at 400 nm is absorbed by the SWNT by about 50%, the remaining about 30% was quenched by the interaction of $^1C_{60}$* with SWNT due to the excited state events.

(23) D' Souza, F.; Deviprasad, G. R.; El-Khouly, M. E.; Fujitsuka, M.; Ito, O. *J. Am. Chem. Soc.* **2001**, *123*, 5277−5284.

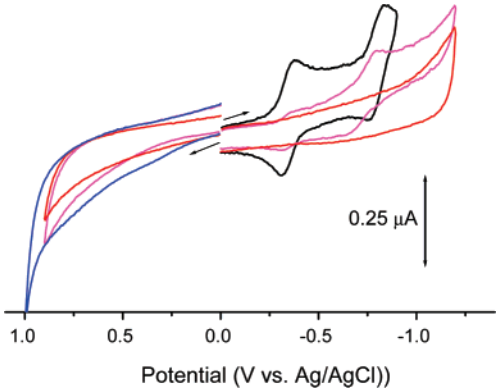

Figure 3. Cyclic voltammograms of (a) crown-C_{60} (dark line), (b) SWNT/Pyr-NH_3^+ (blue line) and (c) SWNT/Pyr-NH_3^+/crown-C_{60} nanohybrids (magenta line) in DMF containing 0.1 M (n-Bu_4N)ClO_4. Scan rate = 0.1 V s^{-1}. The voltammograms shown in red represent solvent background.

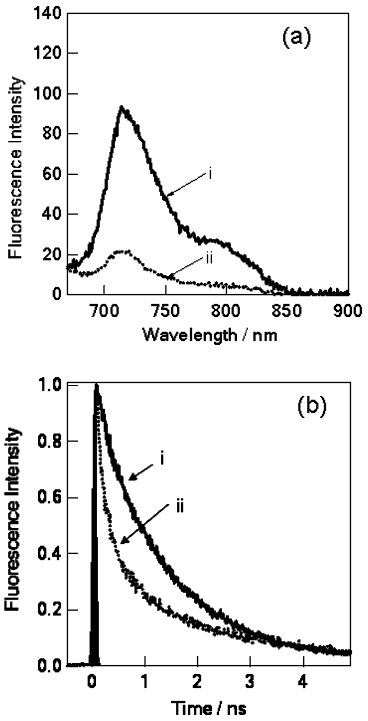

Figure 4. (a) Steady-state fluorescence spectra and (b) time-resolved fluorescence emission decays of crown-C_{60} (i) in the absence and (ii) in the presence of SWNT/Pyr-NH_3^+ in DMF; λ_{ex} = 400 nm. The concentration of crown-C_{60} was held constant at 0.1 mM.

crown-C_{60} hybrid in dilute DMF), which was suggested by the presence of the longer fluorescence lifetime of $^1C_{60}$* in a fraction of ca. 30%. The rise of $C_{60}^{\bullet-}$ around 1020 nm was estimated to be fast within the nanosecond laser pulse (6 ns) (see the time profile in Figure 5 inset), which corresponds to the charge separation within 250 ps as estimated from the $^1C_{60}$*-fluorescence lifetime. The decay of $C_{60}^{\bullet-}$ around 1020 nm mostly finished within 400 ns. From the decay of the $C_{60}^{\bullet-}$, the k_{CR} value of SWNT$^{\bullet+}$/Pyr-NH_3^+/crown-$C_{60}^{\bullet-}$was evaluated to be 1.04 × 10^7 s^{-1}. Using the k_{CR} value, the lifetime of the radical ion-pair, τ_{RIP} (=$1/k_{CR}$) was evaluated to be ca. 100 ns, which is almost the same as porphyrin-crown-C_{60} supramolecules,[13] indicating charge stabilization to some extent in the supramolecular nanohybrid in DMF.

To further confirm the occurrence of charge separation leading to the formation of SWNT$^{\bullet+}$/Pyr-NH_3^+/crown-$C_{60}^{\bullet-}$ in the

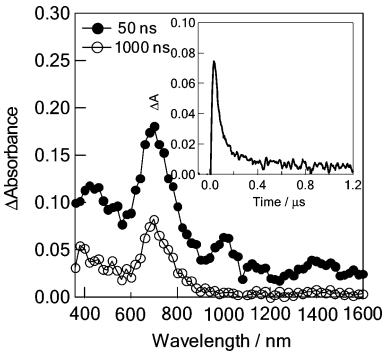

Figure 5. Nanosecond transient absorption spectra of SWNT/Pyr-NH_3^+/crown-C_{60} nanohybrids (0.1 mM) observed by the 532 nm (ca. 3 mJ/ pulse) laser irradiation in DMF. (Inset) Absorption-time profile of the 1020 nm band.

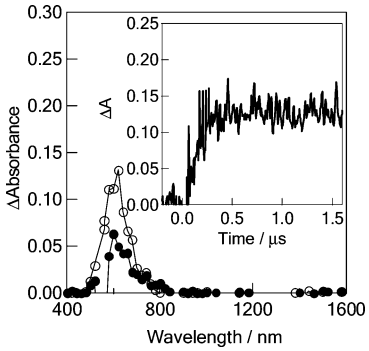

Figure 6. Nanosecond transient absorption spectra of SWNT/Pyr-NH_3^+/crown-C_{60} (0.1 mM) in the presence of 0.5 mM HV^{2+} and 1.5 mM BNAH observed by 532 nm (ca. 3 mJ/pulse) laser irradiation in DMF (at 0.1 μs (●) and 1.0 μs (○)). (Inset) Absorption-time profile of the 620 nm peak.

nanohybrids, electron mediation experiments were performed by the addition of a second electron acceptor, hexyl viologen dication (HV^{2+}), and a sacrificial electron donor, 1-benzyl-1,4-dihydronicotinamide (BNAH), to the solution, and nanosecond transient experiments were performed.[14,24] Because it is easier to reduce viologen compared to C_{60} (see Supporting Information for voltammograms), electron migration from $C_{60}^{\bullet-}$ to HV^{2+} is possible. The oxidation potential of BNAH was reported to be E^0_{ox} = 0.32 V vs Ag/AgCl in benzonitrile,[24] that is, BNAH is much easier to oxidize compared to SWNT. Hence, a hole shift from SWNT$^{\bullet+}$ to BNAH is thermodynamically conceivable. These secondary electron-transfer processes were found to occur as shown in the nanosecond transient absorption spectra of SWNT/Pyr-NH_3^+/crown-C_{60} nanohybrids in the presence of BNAH and HV^{2+} in DMF in Figure 6.

In the presence of HV^{2+} and BNAH, the transient species of SWNT$^{\bullet+}$/Pyr-NH_3^+/crown-$C_{60}^{\bullet-}$ observed in Figure 5 (C_{60} anion radical and triplet state peaks) disappeared, leaving the absorption of radical cation of HV^{2+} ($HV^{\bullet+}$) at 620 nm (Figure 6).[14,24,25] The rise rate of $HV^{\bullet+}$ was evaluated to be 5 × 10^6 s^{-1} from the time profile at 620 nm; thus, the bimolecular rate constant for electron migration from $C_{60}^{\bullet-}$ to HV^{2+} was calculated to be 1 × 10^{10} M^{-1} s^{-1}, which is close to diffusion controlled limit in DMF. The decay of $HV^{\bullet+}$ at 620 nm was prolonged on addition of BNAH, whereas in the absence of BNAH the $HV^{\bullet+}$ species decayed quickly within 100 ns due to

(24) Sandanayaka, A. S. D.; Takaguchi, Y.; Uchida, T.; Sako, Y.; Morimoto, Y.; Araki, Y.; Ito, O. *Chem. Lett.* **2006**, *35*, 1188−1189.
(25) Fukuzumi, S.; Imahori, H.; Okamoti, K.; Yamada, H.; Fujitsuka, M.; Ito, O.; Guldi, D. M. *J. Phys. Chem. A* **2002**, *106*, 1903−1908.

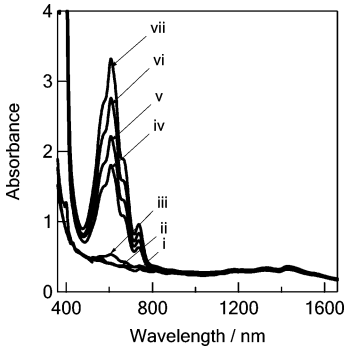

Figure 7. Steady-state absorption spectra of (i) SWNT/Pyr-NH_3^+/crown-C_{60} and (ii) in the presence of 0.5 mM HV^{2+}; after repeated 532-nm laser light irradiation (ca. 3 mJ/pulse) in the presence of [BNAH] = (iii) 0 (yellow), (iv) 0.5 (brown), (v) 0.75 (red), (vi) 1.0 (blue), and (vii) 1.5 mM (black) in deaerated DMF (0.5 cm cell length). The 532-nm laser light was irradiated until maximal concentration was obtained in each system.

electron−hole recombination between $HV^{\bullet+}$ and $SWNT^{\bullet+}$. The slow decay of $HV^{\bullet+}$ is attributed to a disturbance of the back electron transfer, which can be caused by a hole shift process from $SWNT^{\bullet+}$ to BNAH, vanishing $SWNT^{\bullet+}$. Instead, the generated radical cation of BNAH ($BNAH^{\bullet+}$) quickly dissociated into 1-benzyl-nicotinamidinium cation (BNA^+) via deprotonation.[25] That is, stoichiometrically BNAH acts as a two-electron donor to shift two equivalent holes from $SWNT^{\bullet+}$.[26] Disappearance of the absorption of $^3C_{60}$* at 700 nm may be caused by the direct electron transfer from BNAH to unbound crown-$^3C_{60}$*, generating $BNAH^{\bullet+}$ and $C_{60}^{\bullet-}$, which produces additional $HV^{\bullet+}$.

2.7. Electron Pooling Experiments. By the steady-state absorption spectral measurements with the light irradiation in visible wavelength region (532 nm), which predominantly excites the crown-C_{60} and SWNT but not additives (HV^{2+} and BNAH) or Pyr-NH_3^+, the accumulation of $HV^{\bullet+}$ was observed as shown in Figure 7. The concentration of the accumulated $HV^{\bullet+}$ species increased with the BNAH concentration, supporting the role of BNAH as a sacrificial hole shifting reagent.[14,24−26] This observation implies occurrence of photoinduced electron pooling by the excitation of SWNT/Pyr-NH_3^+/crown-C_{60} with the visible light in the presence of HV^{2+} and BNAH. The overall maximal absorbance of $HV^{\bullet+}$ was observed in the presence of 1.5 mM BNAH; thus, maximal concentration of $HV^{\bullet+}$ was evaluated to be 0.2 mM, which amounts to 40% conversion of added HV^{2+} (0.5 mM).

The mechanism for this electron-pooling process can be understood by the C_{60}-fluorescence quenching and transient absorption spectral measurements generating $C_{60}^{\bullet-}$ in the nanohybrids. The $C_{60}^{\bullet-}$ formed upon photoinduced charge-separation in the SWNT/Pyr-NH_3^+/crown-C_{60} nanohybrids, transfers the electron to HV^{2+} generating $HV^{\bullet+}$ as the electron pooling product. The BNAH neutralizes irreversibly the oxidized SWNT in the nanohybrids. These observations of the efficient photosensitized charge-separation/electron-migration/hole-shift processes of the SWNT/Pyr-NH_3^+/crown-C_{60} nanohybrids are illustrated in Scheme 2. In addition to the main processes, which were followed by the fluorescence quenching and transient absorption experimental results, additional processes such as intermolecular electron transfer via unbound crown-$^3C_{60}$* and direct photoexcitation of SWNT, although to a less extent, may also contribute to the overall accumulated $HV^{\bullet+}$.

Scheme 2 [a]

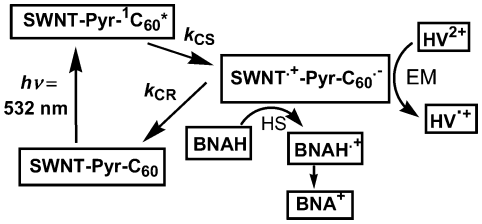

[a] Abbreviations: SWNT/Pyr-NH_3^+/crown-C_{60} = SWNT-Pyr-C_{60}. CS = charge separation, CR = charge recombination, EM = electron migration, and HS = hole shift.

3. Summary

Supramolecular nanohybrids composed of single-wall carbon nanotubes and fullerene were constructed and studied. Both $\pi-\pi$ stacking of pyrene on the SWNT surface, and alkyl ammonium−crown ether interactions were successfully utilized in the self-assembly process. The nanohybrid integrity was probed with various spectroscopic techniques in addition to TEM images. Detailed electrochemical measurements allowed us to probe the redox properties of the SWNT/Pyr-NH_3^+/crown-C_{60} nanohybrids and also to evaluate the related free-energy changes for electron transfer. Such free-energy calculations suggested the possibility of electron transfer from the singlet excited fullerene to carbon nanotube in the SWNT/Pyr-NH_3^+/crown-C_{60} nanohybrids. Steady-state and time-resolved fluorescence studies revealed efficient quenching of the singlet excited-state of C_{60} in the nanohybrids. Nanosecond transient absorption studies confirmed electron transfer as the quenching mechanism resulting into the formation of $SWNT^{\bullet+}$/Pyr-NH_3^+/crown-$C_{60}^{\bullet-}$ charge-separated state. The rates of charge separation, k_{CS}, and charge recombination, k_{CR}, were found to be 3.46×10^9 and 1.04×10^7 s^{-1}, respectively. The calculated lifetime of the radical ion-pair, τ_{RIP}, was found to be over 100 ns, suggesting charge stabilization in the presently developed supramolecular nanohybrids. The electron pooling experiments offered additional evidence for the occurrence of electron transfer in the SWNT/Pyr-NH_3^+/crown-C_{60} nanohybrids where the conversion of HV^{2+} to $HV^{\bullet+}$ was observed, suggesting usefulness of the present self-assembled nanohybrids in artificial photosynthesis applications.

4. Experimental Section

4.1. Chemicals. Single-wall carbon nanotubes, HiPCO, were from Carbon Nanotech. (Houston, TX). All of the reagents were from Aldrich Chemicals (Milwaukee, WI), whereas the bulk solvents utilized in the syntheses were from Fischer Chemicals. Tetrabutylammonium perchloride, (n-Bu_4N)ClO_4, used in electrochemical studies was from Fluka Chemicals. The synthesis of Pyr-NH_3^+ is given elsewhere.[14]

4.2. Synthesis of *N*-Methyl Benzo-[18-crown-6] Fulleropyrrolidine. To a 200 mg (0.28 mmol) of C_{60} in toluene (200 mL) were added 75 mg (0.84 mmol) of sarcosine and benzo-18-crown-6 (477 mg, 1.4 mmol), and the mixture was refluxed for 2 h. After cooling to room temperature, the solvent was evaporated under reduced pressure. The crude compound was purified on silica gel by column chromatography using toluene/ethylacetate (40:60 v/v) as eluent. Evaporation of the solvent yielded the desired compound as a brown solid. Yield: 100 mg (33%).

(26) Fukuzumi, S.; Koumitsu, S.; Hironaka, K.; Tanaka, T. *J. Am. Chem. Soc.* **1987**, *109*, 305−316.

^{1}H NMR [$CDCl_3$]: δ (in ppm): 7.5−7.35 (m, 1H, phenyl *H*), 6.95−6.84 (m, 2H, phenyl *H*), 4.97 (d, 1H, pyrrolidine *H*), 4.85 (s, 1H, pyrrolidine *H*), 4.28−4.2 (m, 2H, pyrrolidine *H* and crownethylene *H*), 4.18−4.11 (m, 3H, crownethylene *H*), 3.96−3.85 (m, 4H, crownethylene *H*), 3.8−3.64 (m, 12H, crownethylene *H*), 1.59 (s, 3H, -CH_3). UV−vis (in DMF, nm): 325, 431, 702.5. ESI mass (in CH_2Cl_2): calcd, 1087.5; found, [M^+] 1088.1.

4.3. Instrumentation. The UV−visible spectral measurements were carried out with a Shimadzu Model 1600 UV−visible spectrophotometer. NIR measurements were performed on a JASCO UV−vis-NIR spectrophotometer. The steady-state fluorescence emission was monitored by using a Varian Cary Eclipse spectrometer. The ^{1}H NMR studies were carried out on a Varian 400 MHz spectrometer. Tetramethylsilane (TMS) was used as an internal standard. Cyclic voltammograms were recorded on an EG&G PARSTAT electrochemical analyzer using a three-electrode system in DMF containing 0.1 M (*n*-Bu_4N)-ClO_4 as the supporting electrolyte. A platinum button electrode was used as the working electrode. A platinum wire served as the counter electrode and a Ag/AgCl was used as the reference electrode. All the solutions were purged prior to spectral measurements using nitrogen gas.

TEM of the carbon nanotubes were obtained by adding isopropanol and sonicating the suspension for 5 min. Samples were placed onto a carbon-coated copper grid. TEM experiments were performed using a JEOL electron microscope (JEM-2010F FasTEMm FEI) operated at 200 kV with an extracting voltage of 4500 V at Research Resources center, UIC, Chicago. The copper grid (200 mesh, Cu PK/100) was supplied by SPI supplies, U.S.A.

The picosecond time-resolved fluorescence spectra were measured using Ti:sapphire laser (Spectra Physics, Tsunami 3950-L2S; pulse width = 100 fs) and a streak scope (Hamamatsu Photonics C4334−01; response time = 10 ps). The details of the experimental setup are described elsewhere.[27] Nanosecond transient absorption measurements were carried out using the 532-nm laser light of an Nd:YAG laser (Spectra Physics, Quanta-Ray GCR-130, fwhm 6 ns) as an excitation source. For the transient absorption spectra in the VIS-NIR regions, the monitoring light from a pulsed Xe lamp was detected with a Si−PIN photodiode (400−600 nm) and a Ge-avalanche photodiode (600−1600 nm).[27]

Acknowledgment. This work is supported by the National Science Foundation (Grant 0453464) and the Petroleum Research Funds administered by the American Chemical Society.

Supporting Information Available: Steady-state fluorescence spectra of Pyr-NH_3^+ and SWNT/Pyr-NH_3^+ in DMF, differential pulse voltammograms, and schemes for accumulation of $HV^{\bullet+}$ in electron-transfer process. This material is available free of charge via the Internet at http://pubs.acs.org.

JA073773X

(27) (a) Matsumoto, K.; Fujitsuka, M.; Sato, T.; Onodera, S.; Ito, O. *J. Phys. Chem. B* **2000**, *104*, 11632−11638. (b) Komamine, S.; Fujitsuka, M.; Ito, O.; Morikawa, K.; Miyata, T.; Ohno, T. *J. Phys. Chem. A* **2000**, *104*, 11497−11504. (c) Yamazaki, M.; Araki, Y.; Fujitsuka, M.; Ito, O. *J. Phys. Chem. A* **2001**, *105*, 8615−8622. (d) Nakamura, T.; Kanato, H.; Araki, Y.; Ito, O.; Takimiya, K.; Otsubo, T.; Aso, Y. *J. Phys. Chem. A* **2006**, *110*, 3471−3479.